www.czasopisma.pan.pl PAN POLSKA AKADEMIA NAUK www.journals.pan.pl

Arch. Metall. Mater. **62** (2017), 2, 595-601

DOI: 10.1515/amm-2017-0088

A. SZCZOTOK*#, J. PIETRASZEK**, N. RADEK***

METALLOGRAPHIC STUDY AND REPEATABILITY ANALYSIS OF γ' PHASE PRECIPITATES IN CORED, THIN-WALLED CASTINGS MADE FROM IN713C SUPERALLOY

The study describes the influence of a surface modification in cored, thin-walled castings of blades from IN-713C nickel superalloy on γ' phase precipitates. The blades were produced by using the investment casting process in the laboratory conditions as parts for a low-pressure turbine rotor. The microstructural observations of the γ' phase precipitates on the cross sections of the blades were performed. The observations were followed by quantitative metallography evaluation, and finally, a comparison of the precipitates between one blade with the conventionally applied ceramic core and one with the core covered layer contained a surface modifier (5% of $CoAl_2O_4$) was made.

Keywords: IN 713C, superalloy, γ' phase, metallography, statistical analysis

1. Introduction

The γ' (gamma prime), the tiny coherent phase is the key to the superalloy's high temperature strength. The development of nickel-base superalloys for turbine applications has focused on increasing the volume fraction of the γ' phase [1]. Cast polycrystalline nickel-base superalloys are typically composed of γ'-phase coherently precipitated in a face-centred cubic (fcc) matrix, together with eutectic phases and one or more carbide phases. The desired properties and resistance to microstructural changes at high temperatures in these alloys are obtained by all phases with a suitable structure, shape, size and distribution. Among all the microstructural factors, the γ' precipitate morphology plays an important role in influencing the properties of nickel-base superalloys [2]. The mechanical properties of nickel-base superalloys are strongly influenced by the morphology of the strengthening γ' precipitates [3]. The γ' precipitates in Ni-based superalloys should be of optimum size, shape and distribution in order to have the desired properties and resist microstructural changes when performing at high temperatures [4]. According to [5], both the sizes and area fractions of different populations of precipitates are influential and therefore need to be quantified and modeled. The investigated material IN713C is the superalloy known since over 40 years. It is still applied for the aircraft parts because its low price and low density comparing to others nickel-based superalloys [6]. The research conducted under the project [7] confirmed the ability of the surface modifier $CoAl_2O_4$ application in the superalloy casting for obtaining grain of required size. In this study the impact of the $CoAl_2O_4$ on the γ' phase precipitates was analyzed.

2. Materials and methods

The studied blades were cast in the precision foundry of Pratt and Whitney, Rzeszow, Poland. IN713C is a commercially available, a precipitation hardenable, nickel-chromium base cast alloy [8-10]. It is characterized by good castability and stability and high strength, as well as a high ductility at elevated temperatures. Its good creep resistance, remarkable resistance to oxidation and thermal fatigue, as well as outstanding structural stability enable its use in gas turbines.

Two cross-sections were cut off from the each blade, as shown in Figure 1.

Each cross-section for the microstructure observations was cut along the axis of the blade (Fig. 2). As a result, four pieces from each blade were obtained: two pieces with convex surfaces (a pressure side of the airfoil lying close the core marked with M) and two with concave surfaces (a suction side of the airfoil lying close a core marked with B). The influence of the typical ceramic core and the core with the 5% surface modifier on the material of the IN713C superalloy was examined, which is why the surfaces lying close the ceramic cores were observed using a scanning electron microscope Hitachi S-4200 equipped with EDS.

* SILESIAN UNIVERSITY OF TECHNOLOGY, FACULTY OF MATERIALS SCIENCE AND METALLURGY, INSTITUTE OF MATERIALS SCIENCE, 8 KRASINSKIEGO STR., 40-019 KATOWICE, POLAND
** CRACOW UNIVERSITY OF TECHNOLOGY, FACULTY OF MECHANICAL ENGINEERING, DEPARTMENT OF SOFTWARE ENGINEERING AND APPLIED STATISTICS, INSTITUTE OF APPLIED INFORMATICS, AL. JANA PAWLA II 37, 31-864 CRACOW, POLAND
*** TECHNICAL UNIVERSITY OF KIELCE, CENTRE FOR LASER TECHNOLOGIES OF METALS, 7 1000-LECIA PANSTWA POLSKIEGO AV., 25-314 KIELCE, POLAND
# Corresponding author: agnieszka.szczotok@polsl.pl

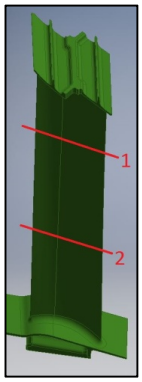

Fig. 1. Scheme of turbine blade with marked cross-sections for research

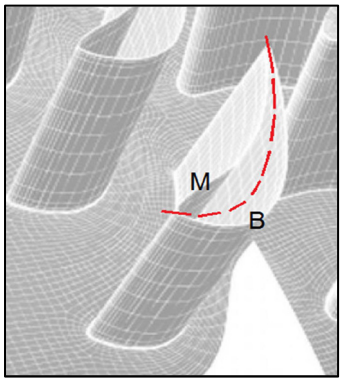

Fig. 2. The way of cutting of cored, thin-walled part of the turbine blade casting

The microstructure of the investigated eight pieces from two castings produced using two kinds of cores was observed on polished and etched metallographic specimens. The specimens were ground and polished with vibratory polishers used for final polishing. The specimens' surfaces prepared in this way were etched with a solution containing: 100 ml H_2O, 100 ml HCl, 100 ml HNO_3 and 3 g MoO_3 by immersion.

The studies which were carried out included a selection of acquisition and image registration parameters. In performed observations, the same image magnification was applied for all the samples in order to compare microstructure in the respective cross-sections.

The recorded microphotographs with γ' phase precipitates were applied for computer-aided image analysis by means of Met-Ilo program [11] to measure and estimate quantitatively the main parameters describing the γ' phase precipitates.

3. Statistical methods

Three input factors, each at two levels, may be distinguished in the experiment:

– TECH, technology (the traditional core and the covered with the 5% modifier),
– HEIGHT, height (labelled by 1 or 2),
– TRACE, surface (labelled by B or M).

The full factorial two-level experimental design leads to 8 different treatments.

Two quantitative outcomes were measured: AREA (the plane section area of the precipitates) and A_A (the area fraction of the precipitates, which is an estimator of their volume fraction).

The analysis started from the fixed-effect model containing linear (main) effects, three two-way interactions and one three-way interaction [12,13]. During the stepwise regression (backward elimination variant) the non-significant terms were eliminated.

The complete results include: the analysis of effects, the Pareto plot of effects, the fixed-effect model and the identification of homogeneous groups of data based on the least significant difference (LSD) test [12]. The conclusion refers to the impact (or the lack of it) induced by the particular input factor.

4. Results

The analyzed material in as-cast state with the application of the traditional core and covered with the 5% modifier contains γ' phase in the form of precipitates, varying in terms of their size

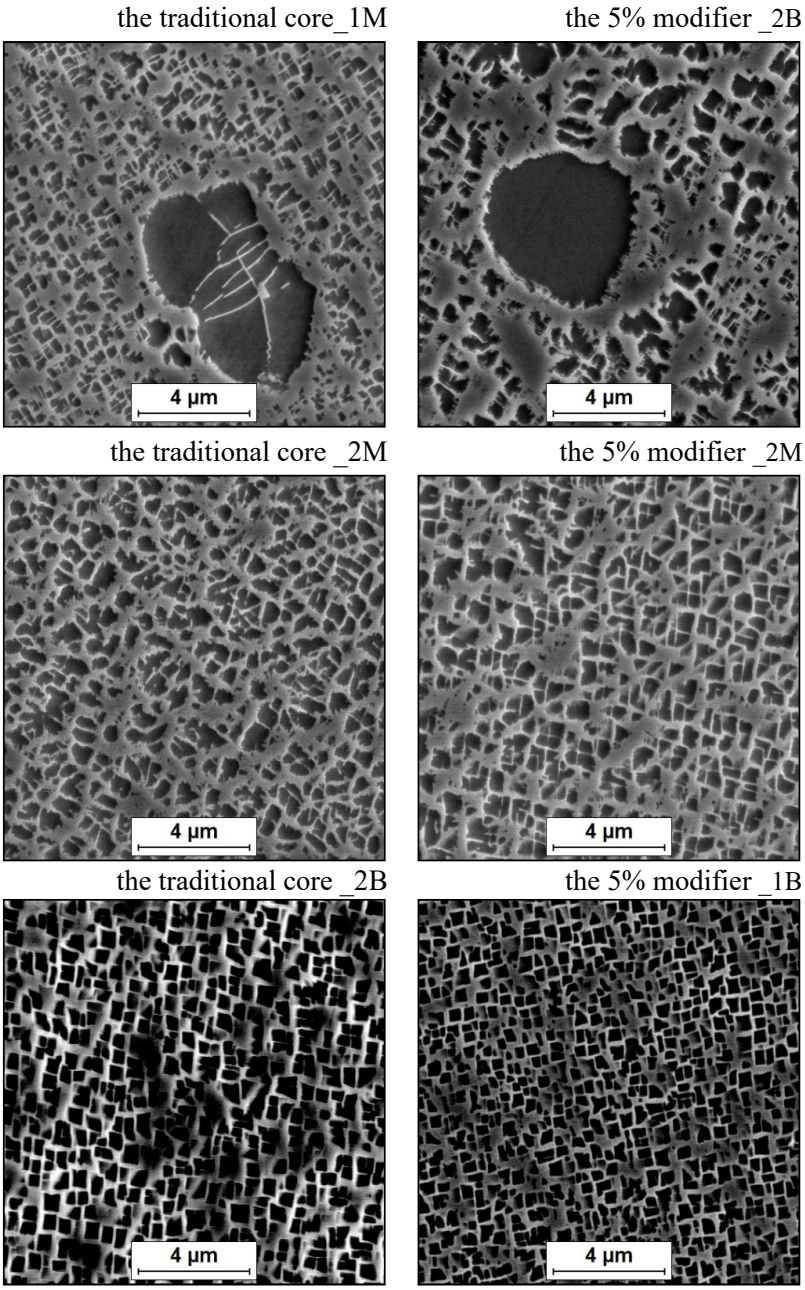

Fig. 3. Characteristic γ' phase precipitates in the IN713C as-cast superalloy in the studied cross-sections with the traditional core and covered with the 5% modifier. SEM, SE

and morphology. It is confirmed in Fig. 3, where examples of γ' phase precipitates at the dendritic cores, within the $(\gamma + \gamma')$ eutectic islands, and at the interdendritic regions were observed.

The quantitative analysis of the γ' phase at the analyzed cross-sections of the turbine blades was limited to the examination of cube-shaped precipitates at the dendritic cores as those having more repetitive morphology and size. It was established that there is a visible difference between the size of γ' phase precipitates in cross-sections with No. 1 and No. 2 both with the traditional and covered with the 5% modifier core (see Figs. 4 and 5). It is the result of the applied feeding system, which was closer to cross-section with No. 2.

To evaluate if the core with the 5% modifier affects size, shape and volume fraction of the γ' phase precipitates performing an image analysis of these precipitates and presenting their description as numerical data is required. The recorded microphotographs with the γ' phase precipitates were applied for the computer-aided image analysis by means of Met-Ilo program [11] to estimate quantitatively the main parameters describing the γ' phase precipitates. A precise quantitative evaluation of the γ' phase precipitates is complicated because of their complex morphology. This requires image processing and analysis methods so as to obtain binary image of the γ' phase precipitates for measurement. An example of the γ' phase precipitates detection was presented in Fig. 6.

An analysis of the γ' phase precipitates was performed by means of traditional quantitative metallography, using image analysis. The analysis of repeatability of the γ' phase precipitates was performed in accordance with the typical statistical methodology [12].

The results of measurements of the γ' phase precipitates are presented in Table 1.

The maximal error of area fraction (A_A) on the basis of the δ error was estimated. The highest value of the maximal error of area fraction (A_A) was 7.57% for the traditional core_2B cross-section. On the grounds of the data in Table 1 we can observe that finer γ' phase precipitates (with smaller values of mean plane section area) there are within cross-sections with No. 1 in the case of the both kinds of cores application. Simultaneously, the γ' phase precipitates within these cross-sections are characterized by higher number of γ' phase precipitates per unit area of plane section, specific length of γ' phase precipitates boundaries and specific surface of γ' phase precipitates boundaries in comparison to cross-sections with No. 2.

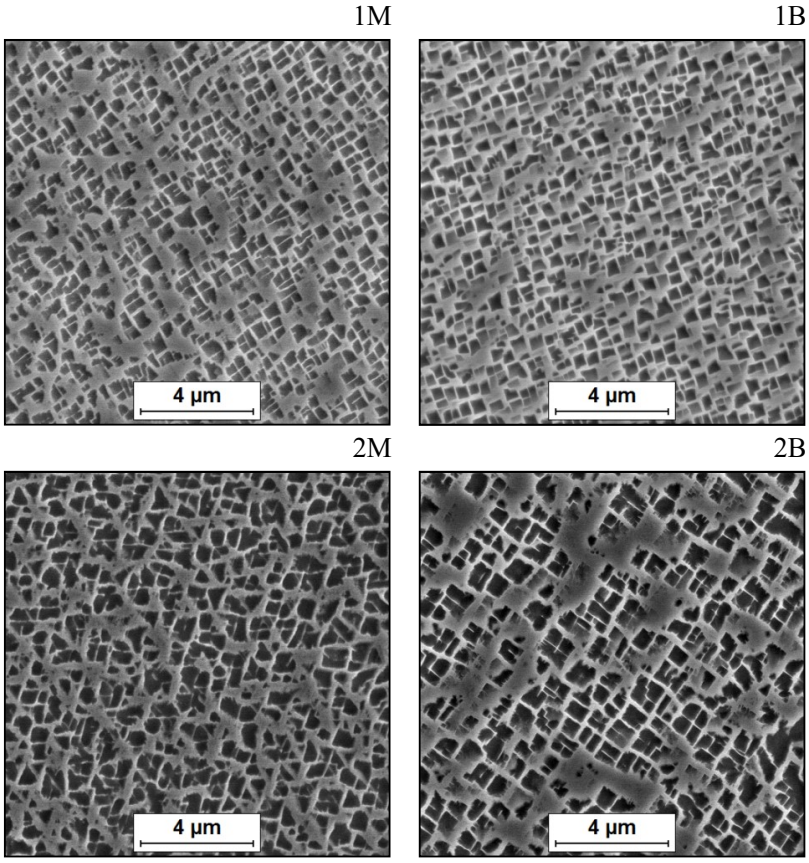

Fig. 4. Microstructure of IN713C superalloy after the traditional core application (selected micrographs from cross-sections). SEM, SE

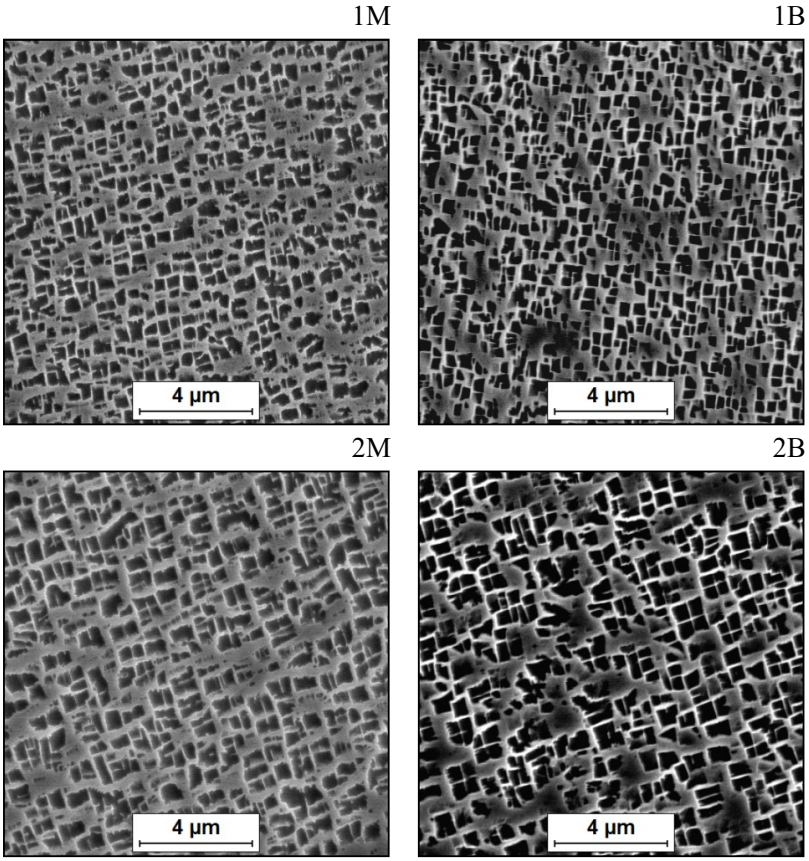

Fig. 5. Microstructure of IN713C superalloy obtained after the core with the 5% modifier application (selected micrographs from cross-sections). SEM, SE

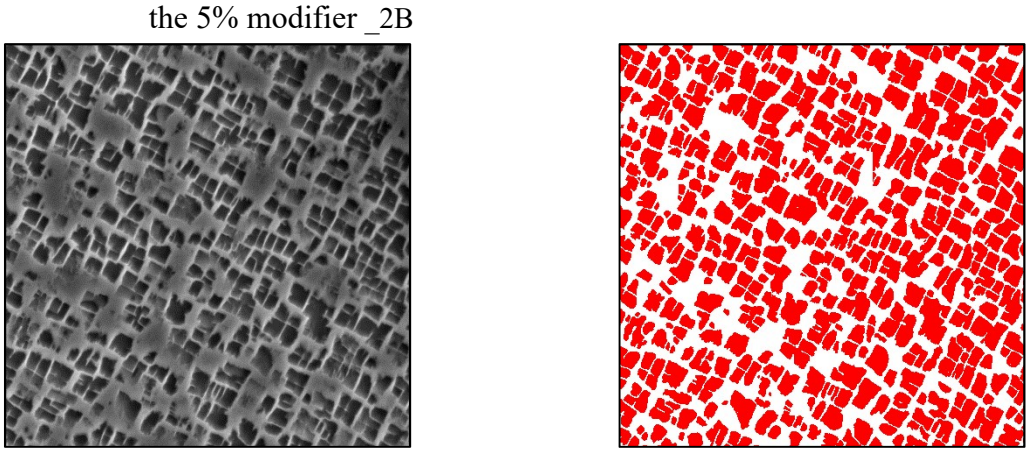

Fig. 6. Microstructure of IN713C superalloy obtained after the core with the 5% modifier application (2B sample) and binary image with detection of the γ' phase precipitates

TABLE 1

The results of measurements of the γ' phase precipitates for the analyzed cross-sections after the traditional and covered with the 5% modifier core application.

Cross-sections	Parameters						
	A_A [%]	$\bar{A}$ [µm^2]	$v(\bar{A})$ [%]	N_A [mm^{-2}]	L_A [mm/mm^2]	S_V [mm^2/mm^3]	δ
the 5% modifier_1B	55.83	0.125	69.46	4425074.3	5627.88	7164.30	0.03
the 5% modifier_1M	55.22	0.121	80.25	4569133.8	5643.51	7184.18	0.03
the 5% modifier_2B	50.21	0.169	76.53	2979042.64	4334.35	5517.62	0.04
the 5% modifier_2M	49.70	0.140	78.84	3540969.66	4664.73	5938.20	0.03
the traditional core_1B	53.31	0.120	65.40	4427792.40	5379.47	6848.07	0.03
the traditional core_1M	56.28	0.112	89.08	5039365.93	5788.09	7368.23	0.03
the traditional core_2B	49.69	0.157	86.04	3172028.07	4476.27	5698.29	0.04
the traditional core_2M	51.56	0.148	86.65	3492764.41	4632.87	5897.65	0.04

where: A_A – area fraction, $\bar{A}$ – mean plane section area, $v(\bar{A})$ – coefficient of variation of plane section area, N_A – number of γ' phase precipitates per unit area of plane section, L_A – specific length of γ' phase precipitates boundaries, S_V – specific surface of γ' phase precipitates boundaries, δ – absolute error of measurement of plane section area of γ' phase precipitates.

Statistical Analysis of A_A

The outcomes were measured at 8 different treatments, each with 2 replications.

The analysis of effect revealed that only the HEIGHT factor affects significantly the outcome A_A (see Table 2), which is indicated by p less than 0.05. All other factors have an insignificant impact on the outcome A_A.

TABLE 2

Analysis of effects for the outcome A_A

Term	Effect	*SE*	*t*	*p*
Constant	52.744	0.608	86.7	0.000
(1)Tech	–0.066	1.217	–0.054	0.958
(2)Height	–4.911	1.217	–4.04	0.004
(3)Trace	0.889	1.217	0.730	0.486
1 × 2	0.739	1.217	0.607	0.561
1 × 3	1.524	1.217	1.252	0.246
2 × 3	–0.216	1.217	–0.178	0.863

The same results, however more spectacular, are presented in the Pareto plot of standardized effects (Fig. 7). The vertical line drawn at $p = 0.05$ marks a distinction between significant and insignificant effects.

In such a case, the fixed-effects model is reduced to only one-factor model:

$$A_A = 52.74 - 2.46 \cdot HEIGHT \quad (1)$$

where *HEIGHT* is coded as (–1) for label 1 and (+1) for label 2. The determination factor yielded $R^2 = 0.70$. The residuals passed the test of normality at $p = 0.995$ (Shapiro-Wilk test).

The relationship between HEIGHT and outcome A_A is presented in the marginal means plot (Fig. 8).

Statistical analysis of AREA (Plane section area)

The outcomes were measured at 8 different treatments with different replications at each treatment. The analysis was conducted for the natural logarithm of the raw outcome AREA, because the data are relatively small and the regression model may return non-physical negative values. The substituted outcome was labeled LN(AREA).

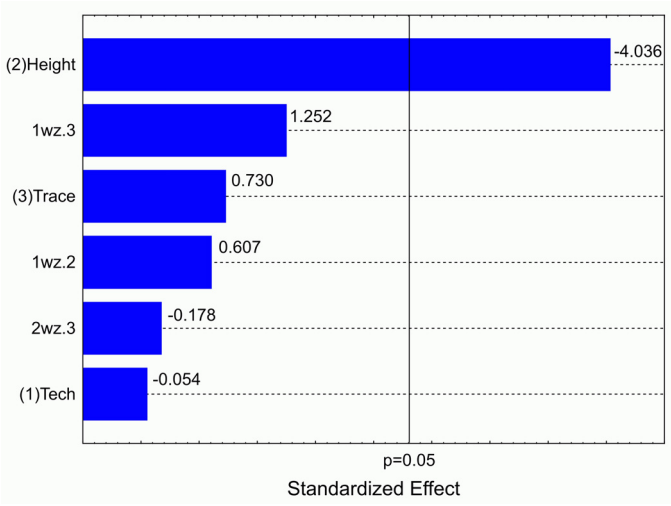

Fig. 7. The Pareto plot of standardized effects for the outcome A_A

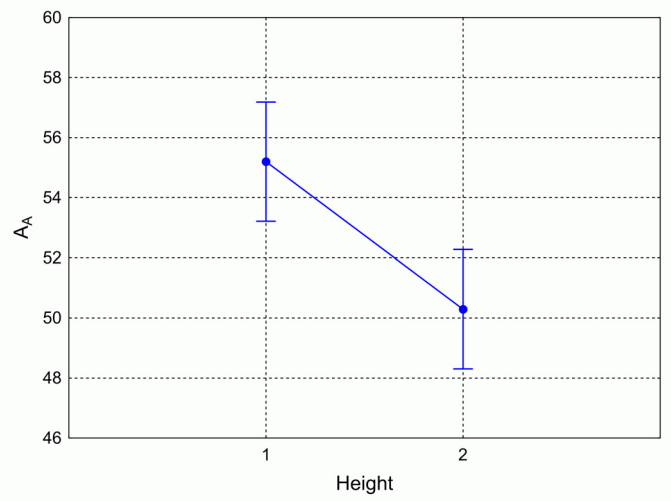

Fig. 8. Marginal means plot for the outcome A_A vs. HEIGHT. The confidence intervals are set for 95%

The analysis of variance revealed that all but the three-way interaction affect LN(AREA) significantly (see Table 3), however interaction term HEIGHTxTRACE has a rather low impact (see Pareto plot Fig. 9). Significant terms are indicated by p less than 0.05.

TABLE 3

Analysis of variance for the outcome LN(AREA)

Term	*SS*	*df*	*MS*	*F*	*p*
Constant	67424.22	1	67424.22	77696.52	0.000
(1)Tech	61.30	1	61.30	70.64	0.000
(2)Height	29.46	1	29.46	33.95	0.000
(3)Trace	157.43	1	157.43	181.42	0.000
1 × 2	12.57	1	12.57	14.48	0.000
1 × 3	11.02	1	11.02	12.70	0.000
2 × 3	4.19	1	4.19	4.82	0.028
1 × 2 × 3	0.03	1	0.03	0.03	0.861
Error	10587.03	12200	0.87		

The same results may be presented in Pareto plot of standardized effects (Fig. 9).

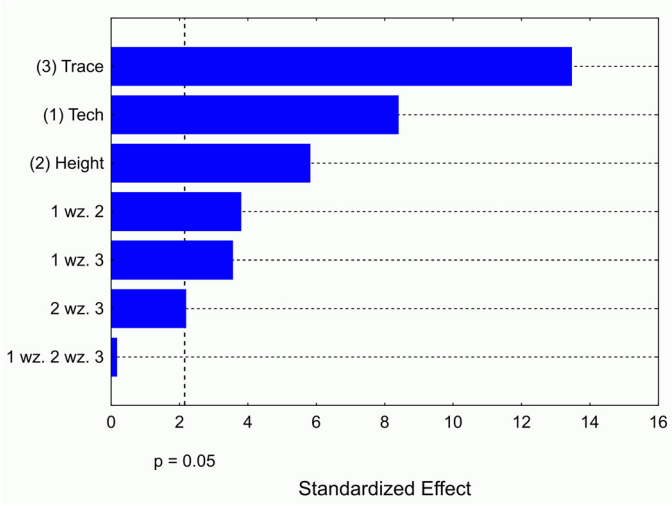

Fig. 9. The Pareto plot of standardized effects for the outcome LN(AREA)

In such a case, the fixed-effects model includes constant, main (linear) effects and all two-way interactions:

$$AREA = EXP\begin{pmatrix} -2.394 + 0.072 \cdot TECH + \\ +0.050 \cdot HEIGHT + 0.116 \cdot TRACE + \\ +0.033 \cdot TECH \times HEIGHT + \\ -0.031 \cdot TECH \times TRACE + \\ +0.019 \cdot HEIGHT \times TRACE \end{pmatrix} \quad (2)$$

where coding is as following:

Factor	–1	+1
TECH	the traditional core	the core covered with 5% modifier
HEIGHT	1	2
TRACE	M	B

The determination factor yielded $R^2 = 0.70$.

In general, the impact of those factors on the LN(AREA) may be presented in Fig. 10, where smaller LN(AREA) relates to smaller AREA.

5. Conclusions

The presented complex procedure of a quantitative evaluation of the γ' phase precipitates of IN 713C superalloy containing a selection of the proper sample preparation, the image acquisition and the image analysis provides obtaining repeatable results.

The results of this investigation suggest that γ' phase precipitates in dendrite cores are characterized by:

- greater mean plane section area in the cross-sections with numbers 2 than in the cross-sections with numbers 1;
- greater volume fraction in the cross-sections with numbers 1 than in the cross-sections with numbers 2.

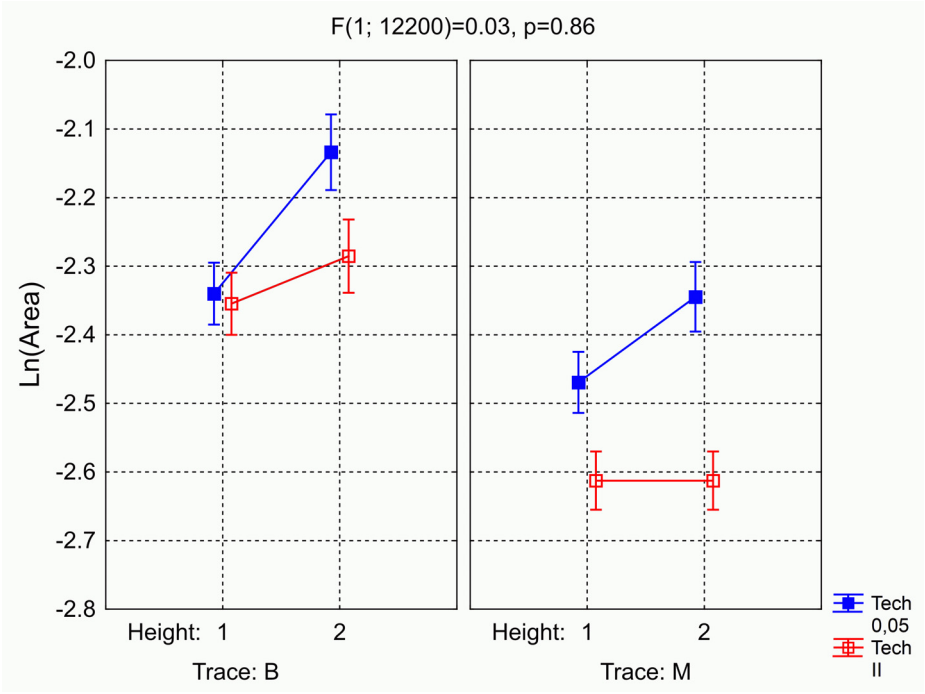

Fig. 10. Impact of three input factors on the outcome LN(AREA)

The type of a technology TECH does not affect the relative volume fraction of the γ' phase precipitates. This outcome depends only on the HEIGHT factor defining the geometrical location of samples (cross-sections).

The type of a technology TECH strongly affects the plane section area of the γ' phase precipitates (AREA), resulting in the larger area of these precipitates, however the impact depends on location defined by factors HEIGHT and TRACE, both defining the geometrical location of samples. The impact is the greatest for the location (HEIGHT=2; TRACE=M), lower and almost mutually equal for locations (HEIGHT=1; TRACE=M) and (HEIGHT=2, TRACE=B), and the lowest and non-significant for location (HEIGHT=1, TRACE=B). In the latter case, the mean area of objects is practically the same for both technologies.

It seems that one should use more sophisticated, but also more computationally expensive statistical non-parametric methods [14-16] in further investigation to reveal relationships between factors deeper than it is possible in a classic statistical analysis [12], however the computational cost of such enhancement is very high [17-18]. If the mesh of samples nodes in the space of factors is sparse, it would rather be explored by a factorial approach [19-21], while if the mesh is dense, the response surface methodology (RSM), particularly with the local approximation, seems to be more appropriate [22-23]. It may include specific non-parametric methods for the analysis of multi dimensional sparse data [24-25], even with a multiphysics approach [26-29], the fuzzy statistics [30-32] for uncertain data or the selection of dominant factors, derived from a production engineering [33].

Acknowledgements

A financial support by the Polish National Centre for Research and Development involved in the carrying-out of Project No. INNOLOT/I/8/NCBR/2013 entitled " Innovative investment casting technologies – INNOCAST" is gratefully acknowledged.

REFERENCES

[1] R.J. Mitchell, M.C. Hardy, M. Preuss and S. Tin: Development of γ' morphology in P/M rotor disc alloys during heat treatment, in: Superalloys 2004 Edited by K.A. Green, T.M. Pollock, H. Harada, TMS (The Minerals, Metals & Materials Society), 2004, 361-370.

[2] H.T. Kim, S.S. Chun, X.X. Yao, Y. Fang, J. Choi: Gamma prime (γ') precipitating and ageing behaviours in two newly developed nickel-base superalloys, Journal of Materials Science **32**, 4917-4923 (1997).

[3] N.S. Stoloff, Fundamentals of Strengthening, in: Superalloys II, C.T. Sims, N.S. Stoloff, W.C. Hagel (eds.), John Wiley & Sons, New York, 61-96, NY, 1987.

[4] A.K. Dwarapureddy, Thesis: Study of particle growth and breakdown in single size gamma prime distribution and high temperature creep in IN738LC nickel superalloy, Louisiana State University and Agricultural and Mechanical College, 2006.

[5] T.P. Gabb, D.G. Backman, D.Y. Wei, D.P. Mourer, D. Furrer, A. Garg, D.L. Ellis, γ' formation in a nickel-base disk superalloy, in: Superalloys 2000, T.M. Pollock, R.D. Kissinger, R.R. Bowman, K.A. Gmn, M. McLean, S. Olson, and J.J. Schirra (Eds.), TMS (The Minerals, Metals &Materials Society) 405-414, 2000.

[6] Alloy Index Vacuum-Melt Alloys, Cannon-Muskegon Group, 3rd ed., 2007.

[7] Reports under the Project No. INNOLOT/I/8/NCBR/2013 entitled "Innovative investment casting technologies – INNOCAST", Silesian University of Technology, Katowice, Poland, 2016.

[8] C.R. de FariasAzevedo, M.F. Moreira, E. Hippert, Nickel superalloy (Inconel 713C). Instituto de Pesquisas Tecnológicas, São Paulo, 2001.

[9] J.F. Radavich, Effects of Zr variations on the microstructural stability of alloy 713C, in: Superalloys 1968, M.J. Donachie Jr. (Ed.), TMS 199-226, 1968.

[10] F. Zupanič, T. Bončina, A. Križman, Mater. Sci. Technol. **18**/7, 811-819 (2002).

[11] J. Szala, J. Cwajna, Acta Stereol. **18**/1, 89-94 (1999).

[12] L. Davies, U. Gather, Robust Statistics. Analysis of Variance., in: J.E.Gentle, W.K. Hardle (Eds.), Handbook of Computational Statistics. Springer-Verlag, Berlin-Heidelberg, 2012.

[13] S.E. Maxwell, H.D. Delaney, Designing experiment and analyzing data: a model comparison perspective. Taylor and Francis, New York, 2004.

[14] J. Pietraszek, E. Skrzypczak-Pietraszek, Adv. Mat. Res. **874**, 151-155 (2014).

[15] J. Korzekwa, A. Gadek-Moszczak, M. Bara, Prakt. Metallogr. Pr. M. **53**, 36-49 (2016).

[16] J. Pietraszek, M. Kolomycki, A. Szczotok, R. Dwornicka, in: N.T. Nguyen, Y. Manolopoulos, L. Iliadis, B. Trawinski (Eds.), Computational Collective Intelligence, ICCCI 2016, Pt I, 260-268, 2016.

[17] A.B. Owen, Empirical Likelihood, Chapman & Hall/CRC, Boca Raton, 2001.

[18] Y. Pawitan, In All Likelihood: Statistical Modelling and Inference Using Likelihood. Clarendon Press, Oxford, 2001.

[19] E. Skrzypczak-Pietraszek, J. Pietraszek, Chem. Biodivers. **11**, 562-570 (2014).

[20] O. Kempthorne, K. Hinkelmann, Design and analysis of experiments. Vol.1. Introduction to experimental design. John Wiley & Sons, Hoboken, NJ, USA, 2007.

[21] S. Ghosh, D. Dimiduk, Computational Methods for Microstructure-Property Relationships. Springer, New York, 2001.

[22] N. Radek, A. Sladek, J. Broncek, I. Bilska, A. Szczotok, in: A. Szczotok, J. Pietraszek, N. Radek, A. Gadek-Moszczak (Eds.), Adv. Mater. Res. **874**, 101-106 (2014).

[23] A. Szczotok, Materialwiss. Werkst. **46**, 320-329 (2015).

[24] R. Dwornicka, Adv. Mater. Res.-Switz. **874**, 63-69 (2014).

[25] I. Dominik, J. Kwasniewski, K. Lalik, R. Dwornicka, 32nd Chin. Contr. Conf., 7505-7509 (2013).

[26] A. Tiziani, A. Molinari, J. Kazior, G. Straffelini, Powder Metall. Int. **22**, 17-19 (1990).

[27] F. Deflorian, L. Ciaghi, J. Kazior, Werkst. Korros. **43**, 447-452 (1992).

[28] T. Lipinski, Solid StatePhenomena **163**, 183-186 (2010).

[29] P. Szabracki, T. Lipinski, Solid StatePhenomena **203-204**, 59-62 (2013).

[30] A. Calcagni, L. Lombardi, E. Pascali, Soft Computing **20**, 749-762 (2016).

[31] J. Pietraszek, A. Sobczyk, E. Skrzypczak-Pietraszek, M. Kolomycki, Technical Transactions **113** (14), 119-125 (2016).

[32] A. Parchami, S.M. Taheri, B.S. Gildeh, M. Mashinchi, in: C. Kahraman, O. Kabak (Eds.), Fuzzy Statistical Decision-Making: Theory and Applications, 155-173 (2016).

[33] J. Pietraszek, M. Krawczyk, A. Sobczyk, E. Skrzypczak-Pietraszek, Technical Transactions **113** (14), 95-100 (2016).